45. *DATA REPORT:* PHYSICAL PROPERTIES OF MASSIVE SULFIDE FROM SITE 856, MIDDLE VALLEY, NORTHERN JUAN DE FUCA RIDGE[1]

Henrike M. Gröschel-Becker,[2] Earl E. Davis,[3] and James M. Franklin[4]

ABSTRACT

The results of eight high-pressure velocity experiments and eight divided-bar thermal-conductivity measurements on massive sulfide samples recovered from Ocean Drilling Program Holes 856G and 856H are presented. Densities, porosities, velocities, and thermal conductivities are highly variable owing to textural and mineralogical variations and the highly porous nature of most of the five types of sulfide reported on here. Porosity occurs as open to partially filled intergranular spaces, vugs, veins, cracks, and fractures. Sulfide samples are not ideal for either high-pressure velocity experiments or divided-bar thermal-conductivity measurements; limitations and sources of potential error are discussed in the text. Sample geometry and textural makeup particularly caused problems in the velocity experiments. The lack of a suitable shipboard high-conductivity standard also contributed to errors, as is apparent from a comparison of the shore-based divided-bar data with shipboard half-space measurements conducted on the same samples. These velocity and thermal-conductivity data, are, to the best of our knowledge, the first to be reported for massive sulfides in the open literature.

INTRODUCTION

The penetration of more than 159 m of massive sulfide at Bent Hill, Middle Valley, at Ocean Drilling Program (ODP) Holes 856G and 856H provided an unusual opportunity for the study of the physical properties of a deposit that probably precipitated at and above the seafloor. Compressional (V_p)- and shear (V_s)-wave velocities of eight oriented massive sulfide minicore cylinders were measured at varying confining pressures using a pulse-transmission technique similar to that of Birch (1960, 1961). Two samples were from Hole 856G and six were from Hole 856H (Table 1). Bulk densities (ρ_b) and porosities were also determined. Results are presented for a Hole 856G/Hole 856H composite section since the two boreholes were drilled no more than 20 m apart (Shipboard Scientific Party, 1992b). A shore-based divided-bar apparatus was used to obtain thermal conductivities of eight 2-cm^3 cubes of massive sulfide cut for shipboard physical properties measurements (Table 2).

SAMPLE DESCRIPTION

Samples are described according to the sulfide classification scheme developed aboard the ship (Figs. 87 and 88, Shipboard Scientific Party, 1992b). Velocity measurements were conducted on two type 1 samples (homogenous, massive, fine-grained pyrrhotite), two type 4 samples (heterogenous and veined, coarse-grained pyrite-pyrrhotite), and four type 5 samples (massive colloform and vuggy pyrite). Thermal conductivities were determined for two cubes of type 4, two of type 5, two of type 2 (homogeneous, massive, fine-grained pyrite-pyrrhotite), and two of type 3 (homogeneous, medium- to coarse-grained pyrite-pyrrhotite).

The average grain density (ρ_g) of our samples is high (4.52 g/cm^3). Variable proportions of pyrite ($\rho_g = 4.92$ g/cm^3), pyrrhotite ($\rho_g = 4.55$ g/cm^3), and magnetite ($\rho_g = 5.15$ g/cm^3) (Horai, 1971), 10%–25% of which is present in type 4 and 5 rocks, result in high ρ_g and ρ_b values. Successive replacement of "primitive" type 1 sulfide to "mature" type

4 and type 5 sulfide occurs through progressive dissolution, replacement, and reprecipitation of primary pyrrhotite with pyrite, chalcopyrite, sphalerite, and magnetite (Shipboard Scientific Party, 1992b). Chalcopyrite and sphalerite have considerably lower grain densities (4.09 and 4.10 g/cm^3, respectively), than the other sulfide minerals (Horai, 1971), are common as late-stage, coarse-grained crystals in type 4 sulfide and, with abundant veining, cause its heterogenous, commonly porous, texture. In contrast, the typical reticulate boxwork texture of type 5 sulfide, with prismatic pores of 0.1–2.0 mm diameter, results from pyrite precipitated after dissolution of precursor sulfide. Open vugs 2–4 mm in diameter commonly comprise up to 10% of this sulfide type. Pyrite dominates, and other sulfides are minor. Open porosity of up to 50% by volume occurs in type 1 sulfide as a consequence of interpenetrating fine-grained blades of dominant pyrrhotite. Chalcopyrite and sphalerite are ubiquitous and occur interstitially to the pyrrhotite and minor (usually less than 10%) pyrite. Percentages of nonopaque minerals, including green smectite, chlorite, amorphous silica, and carbonate, occur interstitially most commonly in types 1–3 and also are present as vein and vug infill in types 4 and 5, where white amorphous silica and chlorite typically form 15% of the rock.

METHODS

Velocity experiments were performed on oriented minicores in the Rosenstiel School of Marine and Atmospheric Science (RSMAS) Petrophysics Laboratory at hydrostatic pressures from 3 to 100 MPa. Wet-bulk densities and porosities were also obtained. Sample preparation and experimental methods were generally the same as those described in Gröschel-Becker et al. (this volume). Preparation of the samples was difficult owing to textural variations and surface irregularities, especially for type 5 (massive colloform and vuggy) sulfides. The polishing required before the samples were loaded into the velocimeter varied from minimal for relatively soft pyrrhotite-rich samples to extensive for the hard, dense, massive pyrite.

Thermal conductivities of oriented cube samples were measured on a divided-bar apparatus at the Pacific Geoscience Centre (PGC) following the general procedures outlined in Davis and Seemann (this volume). Cross-sectional areas and thicknesses of all samples were derived from caliper measurements of the cubes. A minor amount of polishing was done on sample faces to ensure good thermal contact. Samples with broken edges or corners were not included in the study.

Table 1. Variations in densities and compressional- and shear-wave velocities for massive sulfide minicore samples from Holes 856G and 856H.

Core, section, interval (cm)	Direction	Rock type	Density (g/cm³)	Mode	Velocity (m/s)										Pressure (MPa)
					10	20	30	40	50	60	70	80	90	100	
139-856G-															
7R-4, 15–17	h	5:Py	3.86	P	4990	5020	5050	5070	5080	5100	5150	5150	5130	5120	
				S1	2710	2750	2790	2860	2960	3050	3120	3120	3120	3120	
7R-4, 18–20	v	5:Py	4.00	P	6950	7100	7150	7180	7200	7230	7250	7280	7300	7300	
				S1	3510	3540	3610	3650	3710	3780	3830	3840	3800	3770	
				S2	3650	3670	3720	3750	3780	3820	3860	3870	3840	3830	
139-856H-															
3R-1, 18–21	v	4:Py/Po	4.01	P	5860	5900	5940	5970	5990	6030	6060	6080	6090	6120	
				S1	3270	3310	3320	3340	3350	3360	3380	3390	3390	3390	
				S2	3180	3200	3240	3250	3260	3280	3300	3300	3310	3310	
3R-1, 24–27	h	4:Py/Po	3.90	P	5890	5970	6000	6030	6060	6090	6120	6140	6150	6150	
				S1	3280	3300	3320	3320	3330	3330	3360	3410	3350	3350	
				S2	3220	3230	3240	3420	3250	3260	3280	3280	3290	3290	
10R-1, 52–55	h	5:Py	3.85	P	6190	6350	6480	6600	6670	6760	6890	6940	6960	6990	
				S1	3500	3530	3570	3680	3640	—	—	—	3660	3680	
				S2	3330	3510	3590	3650	3660	3690	3750	3790	3840	3870	
10R-1, 56–58	v	5:Py	3.49	P	6430	6530	6600	6660	6730	6840	6910	6950	6980	6990	
				S1	3220	3260	3310	3350	3370	3390	3430	3440	3450	3390	
				S2	3210	3230	3250	3260	3290	3300	3400	3460	3460	3370	
15R-1, 16–18	h	1:Po	3.63	P	3170	3220	3310	3350	3420	3450	3450	3460	3490	3500	
				S1	1790	1840	1850	—	1880	1900	1920	1920	1930	1930	
				S2	1580	1660	1740	1780	1860	1890	1900	1900	1910	1920	
15R-1, 20–22	v	1:Po	3.60	P	3350	3400	3460	3500	3540	3580	3600	3630	3650	3670	
				S1	1710	1770	1810	1840	1870	1900	1930	1940	1960	1970	
				S2	1780	1820	1850	1880	1900	1920	1950	1960	1980	1990	

Note: h = horizontal minicore oriented perpendicular to core axis; v = vertical minicore oriented parallel to core axis; Py = pyrite; Py/Po = pyrite/pyrrhotite; Po = pyrrhotite; P = compressional wave; S1 = shear wave propagating perpendicular to minicore alignment direction; S2 = shear wave propagating parallel to minicore alignment direction.

Table 2. Thermal conductivities, porosities, and major constituent minerals of sulfide cubes samples from Holes 856G and 856H.

Core, section, interval (cm)	Piece no.	Depth (mbsf)	Type/lithology	Shipboard porosity (%)	Shipboard thermal conductivity (W/m–K)	PGC thermal conductivity (a + b + c) (W/m–K)
139-856G-						
3R-1, 39	6	17.9	Type 2: homogeneous massive fine-gr. pyrite-pyrrhotite	11.9	6.2	6.8
4R-1, 34	5	27.2	Type 3: homogeneous medium- to coarse-gr. pyrite-pyrrhotite	17.8	3.6	5.9
6R-1, 140	23	47.7	Type 3: homogeneous medium- to coarse-gr. pyrite-pyrrhotite	17.6		7.8
7R-4, 49	5	60.6	Type 5: massive colloform and vuggy pyrite	14.0	7.2	13.4
139-856H-						
3R-1, 16	2	22.3	Type 4: heterogenous and veined coarse-gr. pyrite-pyrrhotite	6.9	3.8	7.3
3R-3, 107	9	25.8	Type 4: heterogenous and veined coarse-gr. pyrite-pyrrhotite	16.8	4.1	5.1
9R-1, 59	8	53.1	Type 5: massive colloform and vuggy pyrite	22.2	6.3	12.1
13R-1, 40	5	71.3	Type 2: homogenous massive fine-gr. pyrite-pyrrhotite	16.8	4.6	6.5

EXPERIMENTAL LIMITATIONS

Massive sulfides are, in general, not ideal samples for high-pressure velocity experiments. Surface irregularities owing to vugs, microcracks, and partially to fully filled veins, prevented optimum contact of the transducers with the cylinder faces and reduced the accuracy of the measurements, especially V_s. The saturating fluid may have partially drained from these porous samples prior to measurement, resulting in lower V_p than expected at saturated conditions for the relatively low pressures used in this study; the effect of saturation on V_s is negligible (Christensen and Salisbury, 1975, and references therein; Bonner and Schock, 1981). These two problems were most apparent in type 5 sulfides. Repeat measurements were not possible because four of eight samples failed at pressures between 70 and 90 MPa. In general, sulfide V_p and V_s results are good to 1% to 2% up to 80 MPa; velocities of intact igneous rocks are good to 1%.

The greatest source of error in the measurement of conductivity of these samples probably arises from thermal contact resistances. A viscous wetting agent was used on the cube faces to reduce this error because the small temperature difference across the highly conductive massive sulfide cubes (on the order of 0.5 K) relative to that across the standard samples of the bar (typically 3–4 K), makes any temperature drop across the imperfect contacts significant. Oriented cubes were cut from split core sections with a twin-blade cut-off saw (Shipboard Scientific Party, 1992a); hence, the two pairs of opposing faces normal to the long core (a) axis and normal to the split core face (b axis) were generally quite parallel (Fig. 1). The greatest nonparallelism occurred between the split face and its opposite side (normal to the c axis); imperfections of most samples could be accommodated by the gimbaled mount of the upper part of the divided-bar apparatus. Repeat measurements were made in several cases where the a-, b-, and c-axis values differed by more than 10% to 20%. No large or systematic differences were observed in the measurements along any of the three axes, and the values given in Table 2 are average values.

RESULTS

Density, Porosity, and Velocity

Wet-bulk densities of the eight velocity samples range from 3.49 g/cm³ to 4.01 g/cm³; the greatest variations occur in type 5 sulfides (Table 1). Porosities are high, from 10.6% in type 4 Sample 139-856H-3R-1, 18–21 cm, to 28.3% in type 5 Sample 139-856H-10R-1,
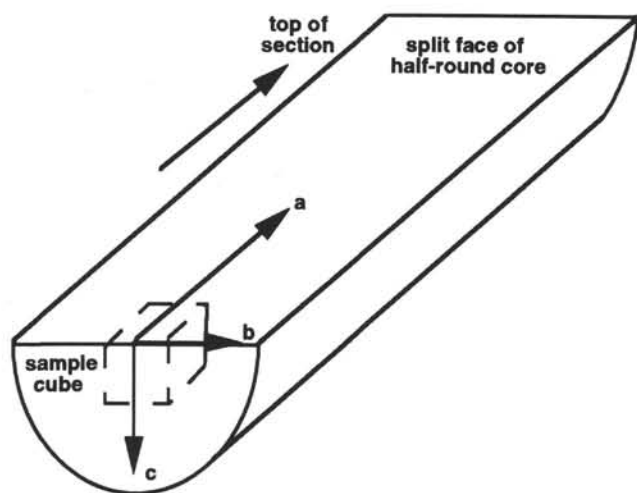
Figure 1. Shipboard convention for orientation of cube samples taken from the working halves of consolidated sediment or hard-rock cores. The a axis is parallel to the vertical axis of the core section, the b axis is across the core parallel to the split core face, and the c axis is through the core perpendicular to the split core face.

56–58 cm (Table 2). The average porosity of type 5 pyrite rocks is 24.7%. Differences in these two properties between adjacent horizontally and vertically oriented sulfide minicores are apparent in Figure 2, which plots wet-bulk density and porosity vs. depth in a Site 856 composite section. Shipboard cube values are plotted for comparison; these and porosity data were recalculated using dry volumes only to be consistent with shore-based values. Density variations of up to 9.9% between nearby samples and observed velocity variations reflect differences in textures, porosity resulting from the prevalence of open and partially filled intergranular pore spaces, vugs, veins, cracks, and fractures, and infilling by nonopaque minerals, as well as variable percentages of sulfide minerals.

Thermal Conductivity

The sulfide conductivities span a large range, from 5.9 to 13.4 W/m–K. The two highest values were measured on samples consisting primarily of pyrite, a mineral that has a particularly high thermal conductivity of 19.2 W/m–K (Horai, 1971). Others contain significant amounts of pyrrhotite, carbonate, silica, and other thermally less conductive minerals, which appears to be the primary reason for their relatively lower conductivities. Detailed petrographic analyses of our samples are needed to analyze the effects of intergranular structure in terms of grain contacts and its relation to conductivity and the systematics of pyrite and other constituent minerals.

Porosities range from 7% to 22%, and although the contrast in thermal conductivity between any of the constituent minerals and water is large, variations in porosity alone cannot account for the variation in conductivity. This is seen clearly in Figure 3, in which the measured thermal conductivities of the samples are plotted against their porosities, as are the relationships predicted by a simple geometric mean mixing law (e.g., Brigaud and Vasseur, 1989) with various constituent mineral conductivities and the conductivity of water of 0.6 W/m–K. The conductivity of 19.2 W/m–K for pure pyrite produces the upper curve; use of a value of 9.0 W/m–K results in a reference curve that provides a crude lower bound for the sulfide data, assuming that the mean harmonic model can be applied. A value of 2.6 W/m–K provides the best fit for the sediment and igneous data. Despite the wide range of implied constituent conductivity values, the minimum value is still high, three times the value inferred from the conductivities and porosities measured on sediment and basalt samples (Davis and Seemann, this volume; shown also in Fig. 3 for comparison).

As is discussed previously, the set-up of the divided-bar apparatus used in this study was not ideal for the measurement of metallic sulfide rocks having high thermal conductivity. The largest source of systematic error is expected to be associated with thermal contact resistance, which would cause values to be erroneously low. An upper limit for the magnitude of such an error can be estimated by calculating the effect of a 0.1-mm gap between the sample and the brass contact plate filled with contact gel having a thermal conductivity of 1 W/m–K. This would introduce an error of 5% into the determination
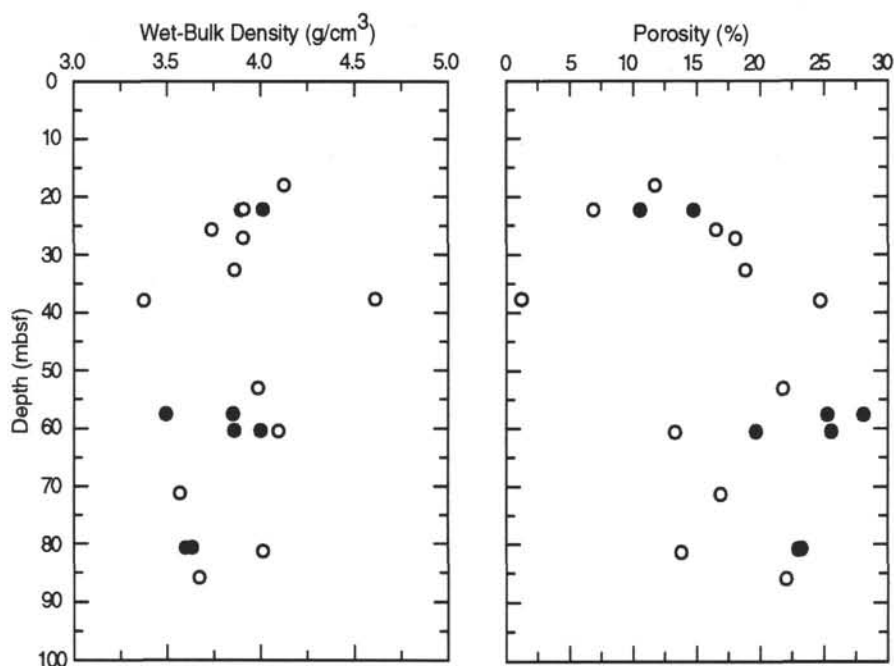

Figure 2. Wet-bulk density vs. depth and porosity vs. depth for a Site 856 composite sulfide section. Filled circles represent data from this study; open circles represent shipboard data.
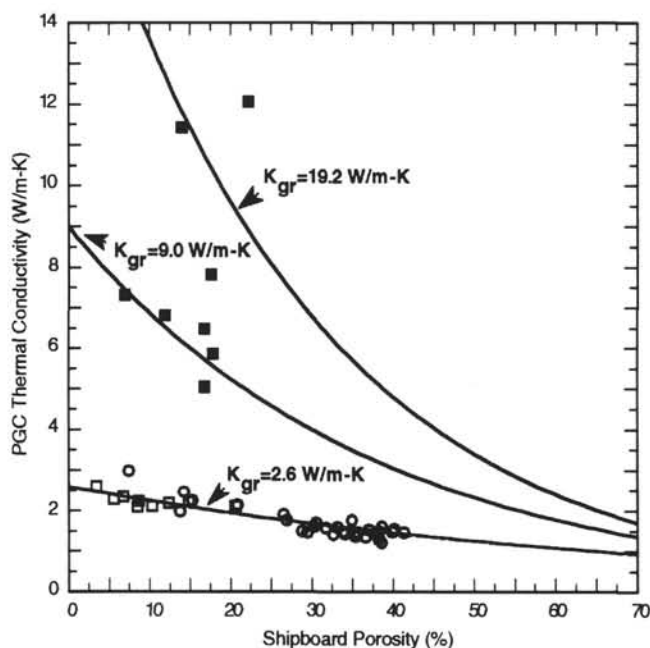
Figure 3. Divided-bar thermal conductivity vs. shipboard porosity for sulfide (filled squares), igneous (open squares), and sedimentary (circles) rocks from Middle Valley. Geometric mean mixing relationships, using three different constituent mineral conductivities (19.2, 9.0, and 2.6 W/m–K) plus water (0.6 W/m–K), are shown as solid lines and are explained in detail in the text. Data for igneous and sedimentary rocks are taken from Davis and Seemann (this volume). Data for sulfide rocks are given in Table 2.
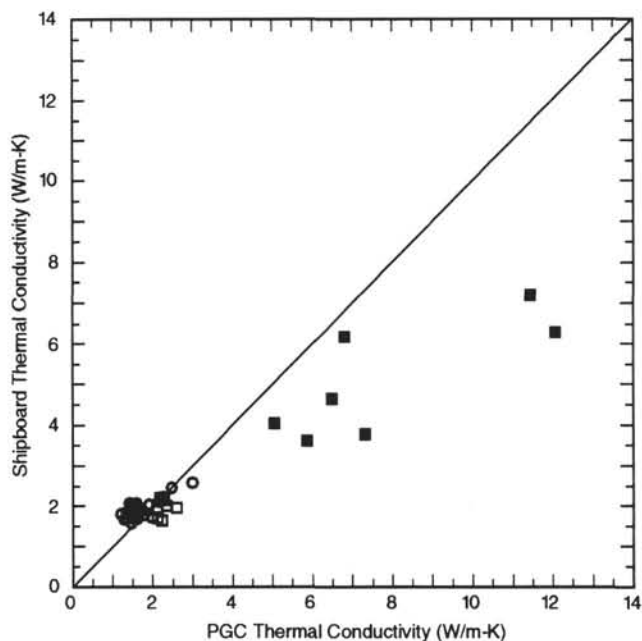
Figure 4. Shipboard thermal conductivity determined with a line source imbedded in a half-space vs. shore-based conductivity determined with a divided bar. Data sources and symbol conventions are the same as in Figure 3.

of the conductivity of a 2-cm^3 rock sample with a conductivity of 10 W/m–K. A comparison of the divided-bar measurements reported here with the line-source shipboard measurements reveals a discrepancy of the opposite sense and of a much larger magnitude (Fig. 4). This result is not surprising, as the method of measuring conductivity with a line-source imbedded in a half-space involves an empirically determined calibration factor determined over a range of conductivities that was limited relative to the values for the sulfide rocks at Site 856 (0.96 to 2.05 W/m–K; Shipboard Scientific Party, 1992a). Concern about this potential source of error was also expressed at the time the shipboard measurements were made (see Shipboard Scientific Party, 1992b). The error associated with this approximation increases with increasing conductivity; shipboard estimates (table 37, Shipboard Scientific Party, 1992b) are roughly half those determined with the divided bar at the highest conductivities. A significant systematic error appears to persist down to values in the region of 3 W/m–K; shipboard values are about 10% lower. No systematic difference exists between measured values below 2 W/m–K, the range over which calibration standards are available.

The velocity and thermal conductivity data, are, to the best of our knowledge, the first to be reported for massive sulfides in the open literature. Electrical resistivity measurements on cube samples are planned.

ACKNOWLEDGMENTS

REFERENCES*

Birch, F., 1960. The velocity of compressional waves in rocks to 10 kilobars, 1. *J. Geophys. Res.*, 65:1083–1102.
————, 1961. The velocity of compressional waves in rocks to 10 kilobars, 2. *J. Geophys. Res.*, 66:2199–2224.
Bonner, B.P., and Schock, R.N., 1981. Seismic wave velocity. In Touloukian, Y.S., and Ho, C.Y. (Eds.), *Physical Properties of Rocks and Minerals:* McGraw-Hill/CINDAS Data Series on Material Properties, II-2:221–256.
Brigaud, F., and Vasseur, G., 1989. Mineralogy, porosity and fluid control on thermal conductivity of sedimentary rocks. *Geophys. J.*, 98:525–542.
Christensen, N.I., and Salisbury, M.H., 1975. Structure and constitution of the lower oceanic crust. *Rev. Geophys. Space Phys.*, 13:57–86.
Horai, K., 1971. Thermal conductivity of rock-forming minerals. *J. Geophys. Res.*, 76:1278–1308.
Shipboard Scientific Party, 1992a. Explanatory notes. In Davis, E.E., Mottl, M.J., Fisher, A.T., et al., *Proc. ODP, Init. Repts.*, 139: College Station, TX (Ocean Drilling Program), 55–97.
————, 1992b. Site 856. In Davis, E.E., Mottl, M.J., Fisher, A.T., et al., *Proc. ODP, Init. Repts.*, 139: College Station, TX (Ocean Drilling Program), 161–281.